



HAL
open science

PEM single fuel cell as a dedicated power source for superconducting coils

Rafael-Antonio Linares-Lamus, Stéphane Raël, Kévin Berger, Melika Hinaje,
Jean Lévêque

► **To cite this version:**

Rafael-Antonio Linares-Lamus, Stéphane Raël, Kévin Berger, Melika Hinaje, Jean Lévêque. PEM single fuel cell as a dedicated power source for superconducting coils. 9th International Exergy, Energy and Environment Symposium (IEEEES-9), May 2017, Split, Croatia. pp.415-421. hal-01540155

HAL Id: hal-01540155

<https://hal.science/hal-01540155>

Submitted on 15 Jun 2017

HAL is a multi-disciplinary open access archive for the deposit and dissemination of scientific research documents, whether they are published or not. The documents may come from teaching and research institutions in France or abroad, or from public or private research centers.

L'archive ouverte pluridisciplinaire **HAL**, est destinée au dépôt et à la diffusion de documents scientifiques de niveau recherche, publiés ou non, émanant des établissements d'enseignement et de recherche français ou étrangers, des laboratoires publics ou privés.

PEM single fuel cell as a dedicated power source for superconducting coils

Linares Rafael, Raël Stéphane, Berger Kévin, Hinaje Melika*, Lévêque Jean

Université de Lorraine, GREEN, Faculté des Sciences et Technologies, B.P. 70 239, Vandoeuvre-lès-Nancy cedex, 54506,

* E-mail: melika.hinaje@univ-lorraine.fr

Abstract

Fuel cells are, in essence, low-voltage energy sources. Moreover, preliminary investigations led with a single proton exchange membrane fuel cell (PEMFC) demonstrated its behavior as a DC current source, in which the current can be directly controlled by the H_2 flow rate for sufficiently low voltage. In this paper, we propose to take advantage of both low voltage level and current source operating mode to supply energy to a high inductance superconducting coil. Due to sensitivity to current ripples among others, at present, superconducting coils supply is dealt with the use of specific electronic power supplies, exhibiting in most cases a huge volume and/or a low energy yield. Since resistance of superconducting coils is zero, this particular use of PEMFC requires to operate in short-circuit, which is unusual in regular approach. For this purpose, we first define requirements of such an application, by making use of a PEMFC electrical model based on a 1D analog representation of mass transport phenomena. This model, which is directly implemented in a standard simulation software used in electrical engineering, enables to take into account the influence of gas supply conditions, notably diffusion limit operation. Then, these theoretical principles are validated by supplying a 10 H superconducting coil cooled by liquid helium by means of a single 100 cm² PEMFC.

Keywords: PEM fuel cell, electrochemical dynamic modeling, mass and charge transport, controlled current source, power supply, high inductance superconducting coil, short-circuited PEMFC

I. Introduction

Polymer electrolyte membrane (PEM) fuel cells are by essence low voltage sources. Indeed, the voltage of an elementary fuel cell (FC), called single cell in the following, is usually near 1 V at open circuit and around 0.6 V at rated conditions of power generation. So that for most practical applications, power management is carried out by fuel cell stacks (series associations of single cells) and electronic converters, allowing in particular to rise the voltage to usual application levels. Moreover, previous theoretical and experimental investigations by Hinaje et al. (2012) led in GREEN laboratory (Groupe de Recherche en Electrotechnique et Electronique de Nancy) with a single PEM fuel cell (PEMFC), either short-circuited or hybridized by discharged supercapacitors, could evidence the electrical behavior as a current source, in which the current is directly controlled by the H_2 flow rate after Faraday's law (NB: for usual FC applications, H_2 is fed in excess in comparison to the current generated). The basic principle is schemed in Fig. 1: at very low voltage operation, close to short-circuit conditions, the cell operating point is situated in the limit diffusion area, which corresponds in electrical theory to an ideal current source. This particular behavior of the cell can be of great interest for specific applications requiring an electrical supply with direct current under a nearly zero voltage.

We propose in this paper an innovative application that takes great advantage of both fuel cell low voltage and current source behavior: the electrical supply for high inductance superconducting coils. Following studies led in GREEN laboratory on FC operation as a current source, previous works

depicted by Hinaje et al. (2013) already report experimental results about the use of a fuel cell for supplying current to a superconducting coil. But it concerns a coil with small inductance value, i.e. 4 mH, which is not representative of the problems and requirements met with big superconducting coils. In this work, a 10 H superconducting coil is supplied by a PEMFC, what has never been achieved before.

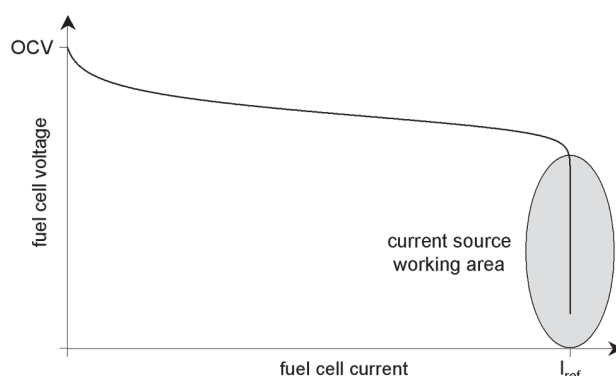


Fig. 1: "PEMFC polarization curve including the area where the cell runs as a current source controlled by H_2 flow rate set by I_{ref} "

At present, such applications are dealt with the use of specific electronic power supplies, exhibiting in most cases a huge volume and/or a low energy yield. Feeding superconducting devices raises a number of constraints, not only because currents can exceed several kA but also because of the very low amplitudes of current oscillations required to avoid transition (persistent variations in the current amplitude generate electrical losses in the superconductor material that can cause the accidental loss of the superconductor state, best

known as quench phenomenon), or even destruction of the coils. Moreover the electronic supplies mentioned above generate harmonic noise onto the industrial grid, and the increase in current to its nominal level has to be achieved carefully. The main advantages to be taken from FCs operated at very low voltages are autonomy (no supply connected to the grid), ensured continuous operation (no risk of power failure due to the grid), together with the electrical quality of the current generated, i.e. free harmonic oscillations. Another great advantage, compared with electronic power supplies for which high currents lead to heavy, bulky and expensive equipments, is that for high power coils, the active area of the electrochemical generator has only to be enhanced, either by connecting single cells in parallel, or by using a single cell whose active area suffices the desired level of current. Of course, the solution proposed here for the generation of the perfectly direct current relies upon a FC fed by H₂ from cylinders, for which safety cautions have to be taken. But operation of superconducting coils, which have to be cooled with liquid nitrogen or helium or by specific cooling gases, represents by itself a really safety-demanding process, which could easily accommodate the presence of a PEMFC. At last, recent works by [Bonnet et al. \(2016\)](#) led in LRGP laboratory (Laboratoire Réactions et Génie des Procédés) have demonstrated that operating a single PEMFC at a voltage far below the threshold recommended by the cell manufacturer does not lead to additional aging, compared with usual operating conditions.

In the first part, we briefly present a PEMFC dynamic model based on an analog formulation of transport partial differential equations (PDE), and implemented in an electrical engineering simulation software. Model is detailed by [Noiying et al. \(2012\)](#). Then, we demonstrate that this model is suitable to simulate a single PEMFC operating as a current source controlled by H₂ flow rate. In the second part, we detail theoretical principles and experimental results, dealing with power superconducting coil supplied by a single PEMFC. The electrical structure is first presented, as well as the experimental bench. Then, we investigate by simulation requirements that enable safe operation of the FC when a huge inductive coil is supplied. Finally, the theoretical principles could be validated, through various experiments with a 100 cm² a single PEMFC and a 10 H superconducting coil.

II. Modeling a PEM single fuel cell operating as a controlled current source

II.1. 1D dynamic PEM single cell model

In previous work led by [Noiying et al. \(2012\)](#), we presented a PEMFC electrochemical model obtained from electrical analogy of mass transport phenomena in gas diffusion layers (GDL) and membrane. This model, which is fundamentally based on transport (PDE), is implemented in simulation software commonly used in electrical engineering to design systems (e.g. Saber, in present case). As a result,

although it can be considered of circuit type, and contrary to most circuit models found in the literature such as those presented by [Yu and Yuvarajan \(2005\)](#), [Andujar et al. \(2008\)](#), [Lazarou et al. \(2009\)](#), [Chiu et al. \(2004\)](#), [Page et al. \(2007\)](#), and [Fontès et al. \(2010\)](#), it naturally includes large signal description, space-dependent parameters (through local partial pressures in GDL, and water content in the membrane), and influence of operating conditions (temperature, gas flow rates, pressure, humidity). In this work, our purpose is to use it for simulating FC operation as an electrical current source controlled by H₂ flow rate, in order to determine requirements for supplying current to a power superconducting coil.

As schemed in Fig. 2, a single PEMFC is composed of a membrane sandwiched between two catalyst layers and two GDLs. We remind hereafter equations that describe gas mixture transport in anode and cathode GDL, water transport in the membrane, double layer phenomena, inlets and interface boundary conditions, electrochemical overvoltages at membrane/electrode interfaces, and ohmic voltage drop across the membrane.

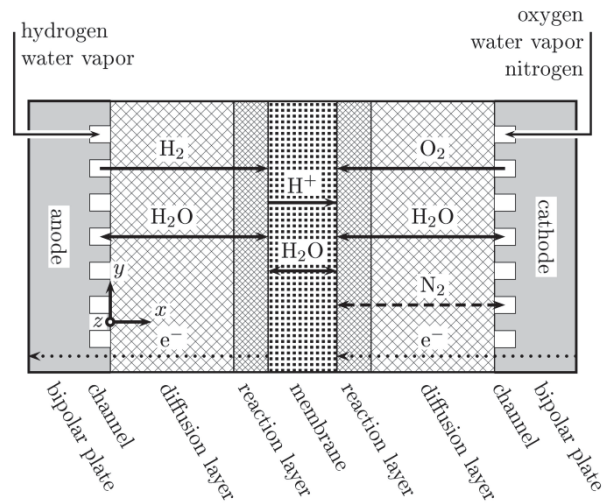


Fig. 2: "Internal structure of a single PEM fuel cell"

Assumptions and simplifications adopted in the present model are as follows:

- 1) the cell temperature is constant and homogeneous,
- 2) gas mixtures are in a single phase,
- 3) mass and charge transports are one-dimensional,
- 4) the membrane is gas-tight, and homogeneous,
- 5) catalyst layers are considered as interfaces.

Both Knudsen and Stefan-Maxwell diffusions are taken into account to describe gas mixture transport in GDLs, so that each gas i (H₂ or H₂O at the anode, O₂ or N₂ or H₂O at the cathode) of the mixture is governed by the following laws:

$$\begin{cases} \frac{\partial P_i}{\partial x} = -\frac{RT}{A_{cell}} \cdot \left(\frac{J_i}{D_{i,eff}} + \sum_{j=1, j \neq i}^N \frac{P_j \cdot J_i - P_i \cdot J_j}{P \cdot D_{ij,eff}} \right) \\ \frac{\partial P_i}{\partial t} = -\frac{RT}{\varepsilon \cdot A_{cell}} \cdot \frac{\partial J_i}{\partial x} \end{cases} \quad (1)$$

where N is the number of species ($N_a = 2$ and $N_c = 3$),

J_i , P_i and $D_{i,eff}$ are the molar flow, the partial pressure and the effective Knudsen diffusion coefficient of the gas i , $D_{ij,eff}$ is the effective Stefan-Maxwell diffusion coefficient of gases i and j , P is the total pressure, and ε is the GDL porosity.

Boundary conditions at membrane-electrode interfaces ($x = \delta_a$ and $x = \delta_a + \delta_m$) are linked to reactant consumption, water production, and water molar flow continuity. This leads at the anode side to:

$$\begin{cases} J_{H_2}(\delta_a) = \frac{I_a}{2F} \\ J_{H_2Oa}(\delta_a) = J_{H_2Om}(\delta_a) \end{cases} \quad (2)$$

and at the cathode side, to:

$$\begin{cases} J_{O_2}(\delta_a + \delta_m) = -\frac{I_c}{4F} \\ J_{N_2}(\delta_a + \delta_m) = 0 \\ J_{H_2Oc}(\delta_a + \delta_m) = J_{H_2Om}(\delta_a + \delta_m) + \frac{I_c}{2F} \end{cases} \quad (3)$$

I_a and I_c being the Faraday components of anodic and cathodic currents, respectively.

Boundary conditions at GDL inlets ($x = 0$ and $x = \delta_a + \delta_m + \delta_c$) can be expressed versus gas relative humidities (HR_a , HR_c), humidifier water temperatures ($T_{hum,a}$, $T_{hum,c}$), gas mixture pressures ($P_{a,in}$, $P_{c,in}$), and gas supply conditions (reference current I_{ref} , reactant stoichiometries ζ_a and ζ_c). This leads at the anode side to:

$$\begin{cases} P_{H_2Oa,in} = HR_a \cdot P_{sat}(T_{hum,a}) \\ P_{H_2,in} = P_{a,in} - P_{H_2Oa,in} \\ J_{H_2,in} = \zeta_a \cdot I_{ref} / (2F) \\ J_{H_2Oa,in} = (P_{H_2Oa,in} / P_{H_2,in}) \cdot J_{H_2,in} \end{cases} \quad (4)$$

and at the cathode side to:

$$\begin{cases} P_{H_2Oc,in} = HR_c \cdot P_{sat}(T_{hum,c}) \\ P_{O_2,in} = 0.21 \cdot (P_{c,in} - P_{H_2Oc,in}) \\ P_{N_2,in} = 0.79 \cdot (P_{c,in} - P_{H_2Oc,in}) \\ J_{O_2,in} = -\zeta_c \cdot I_{ref} / (4F) \\ J_{H_2Oc,in} = (P_{H_2Oc,in} / P_{O_2,in}) \cdot J_{O_2,in} \\ J_{N_2,in} = (P_{N_2,in} / P_{O_2,in}) \cdot J_{O_2,in} \end{cases} \quad (5)$$

Water transport in the membrane is due to both diffusion and electro-osmotic drag. The molar flow of water transported across the membrane is then governed by:

$$\begin{cases} J_{H_2Om} = \frac{n_d}{F} \cdot I_m - A_{cell} \cdot D_{H_2Om} \cdot \frac{\partial c_{H_2O}}{\partial x} \\ \frac{\partial c_{H_2O}}{\partial t} = -\frac{1}{A_{cell}} \cdot \frac{\partial J_{H_2Om}}{\partial x} \end{cases} \quad (6)$$

where J_{H_2Om} is the water molar flux, c_{H_2O} is the water concentration, I_m is the ionic current flowing through the membrane, n_d is the electro-osmotic drag coefficient (number of water molecules dragged per

proton), and D_{H_2Om} is the water diffusion coefficient. As previously mentioned, the continuity of water molar flow is considered at the membrane-electrode interfaces ($x = \delta_a$ and $x = \delta_a + \delta_m$). Moreover, the phase change which takes place for water at these interfaces (vapour phase in GDLs, liquid phase in the membrane) is computed using sorption curves. This enables the calculation of the membrane water content λ at membrane boundaries, versus water activity $a = P_{H_2O} / P_{sat}$ as follows:

$$\begin{cases} \lambda(\delta_a) = \lambda_{sorp} \left(\frac{P_{H_2Oa}(\delta_a)}{P_{sat}(T_{cell})} \right) \\ \lambda(\delta_a + \delta_m) = \lambda_{sorp} \left(\frac{P_{H_2Oc}(\delta_a + \delta_m)}{P_{sat}(T_{cell})} \right) \end{cases} \quad (7)$$

The membrane water content λ is defined versus the membrane proton exchange capacity X_m (number of available sulfonic sites per mass unit), membrane density ρ_m and water concentration by:

$$\lambda = \frac{C_{H_2O}}{X_m \cdot \rho_m} \quad (8)$$

The numerical laws for the various parameters required in the model can be found in [Noiying et al. \(2012\)](#).

By means of space discretization of PDE (1) and (6), both gas mixture transport in GDLs and water transport in the membrane can then be computed using an electrical analogy, for which pressures and water content are assimilated to voltages, and molar flux to currents. Fig. 3 depicts the structure of the model implemented in Saber software. It consists in two parts coupled to each other.

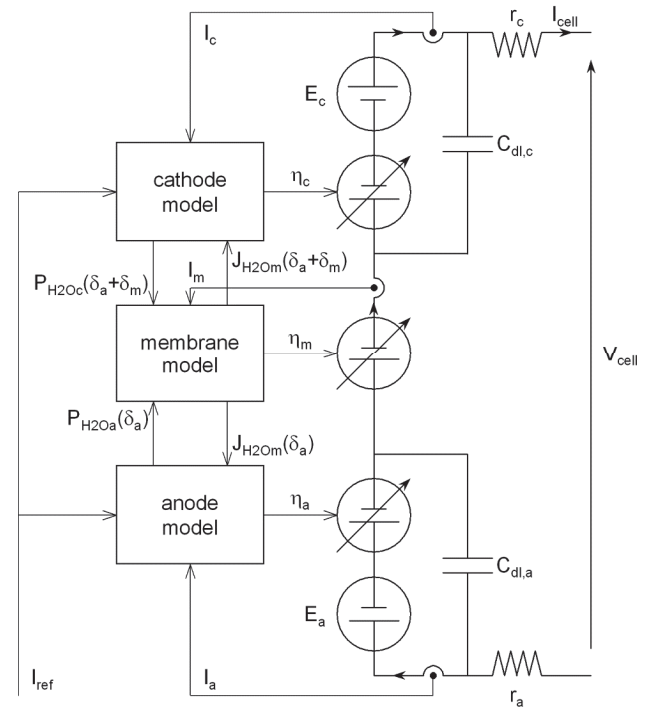


Fig. 3: "PEM fuel cell model: implementation in electrical engineering simulation software by [Noiying et al. \(2012\)](#)"

The first part is dedicated to mass transport and associated variables: gas flows and partial pressures in GDL, water content and water flow in the membrane. Then, electrochemical overvoltages at the membrane/electrode interfaces are calculated using Butler-Volmer law, and the voltage drop across the membrane is deduced from its non-linear ionic resistance (which locally depends on membrane water content).

The second is a standard electrical scheme including double layer capacitors and electronic resistances of both electrodes, in addition to electrochemical interfaces and the membrane. This electrical part of the model computes the FC voltage as a function of FC current, equilibrium potentials, overvoltages (note that these are non ideal voltage sources, so that they can be connected in parallel with double layer capacitors without any resolution trouble), and membrane resistive voltage drop. More details can be found in [Noiying et al. \(2012\)](#) about analog formulations of PDE (1) and (6), about their implementations in Saber software, and about computation of all overvoltages.

II.2. Simulating low voltage operation of a PEMFC model

Fig. 4 shows the FC current obtained when short-circuiting a PEMFC. The dashed blue line is an experimental curve, recorded with a 100 cm² single cell supplied with air and pure dry H₂. The cell temperature, kept at 60 °C, is regulated by a water cooling system. Air is humidified by means of a bubble humidifier. Inlet air temperature is 50 °C, which corresponds to a relative humidity of approximately 60 %. Gas pressure is the ambient level both anode and cathode sides. The inlet gas flow rates are set by a reference current I_{ref} , as follows:

$$\begin{cases} d_{H_2} = \frac{I_{ref}}{2F} \cdot \frac{RT_0}{P_0} \cdot \zeta_a \cdot 1000 \cdot 60 \\ d_{air} = \frac{I_{ref}}{4F} \cdot \frac{RT_0}{P_0} \cdot \frac{1}{0.21} \cdot \zeta_c \cdot 1000 \cdot 60 \end{cases} \quad [\text{L} \cdot \text{min}^{-1}] \quad (9)$$

with $T_0 = 273 \text{ K}$ and $P_0 = 1.013 \cdot 10^5 \text{ Pa}$. In these equations, ζ_a and ζ_c are anode and cathode over-stoichiometric coefficients, respectively. As it can be noticed on the experimental current waveform, the steady state current value is 20 A, from which the H₂ flow rate could be so at the anode inlet. It can also be observed that the FC current first rises strongly, and remains higher than the expected 20 A during several tens of seconds. This transient current overshoot is due to the H₂ stored in the inlet pipe and in GDL during the initial zero current operation that occurs before applying short-circuits.

In Fig. 4, the solid red line presents the current response obtained with the model. The volume of the anode inlet pipe has been represented, in here using electrical analogy, by means of an input capacitor. As it can be seen in the simulated short-circuit current, the model describes correctly the overall experimental

response, including current source operation in steady-state, and transient current overshoot. Both are of major importance to determine the correct H₂ flow rate slope, when supplying current to a huge inductance with a FC.

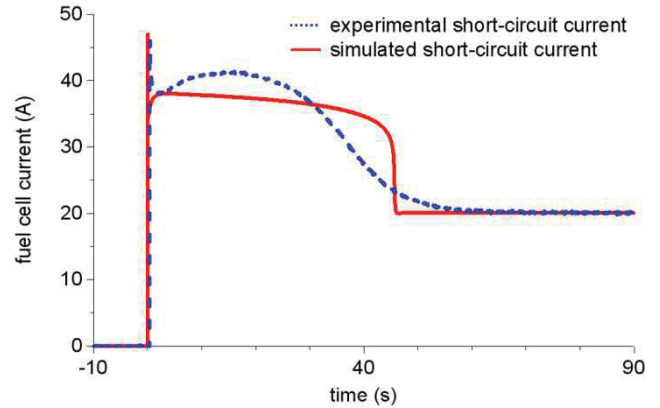


Fig. 4: “Experimental (dashed blue line) and simulated (solid red line) short-circuit of a single PEMFC. Gas flow setting: $I_{ref} = 20 \text{ A}$, $\zeta_a = 1$, $\zeta_c = 4$ ”

III. Supplying a 10 H superconducting coil: principles and experimental results

III.1. Structure of the superconducting coil current supply

The electrical structure is depicted in Fig. 5. It is composed of a 100 cm² single PEMFC, a high current MOS transistor for emergency stop, a superconducting coil with its protection resistor, and a free-wheeling diode (FWD) to ensure current continuity in the inductive coil.

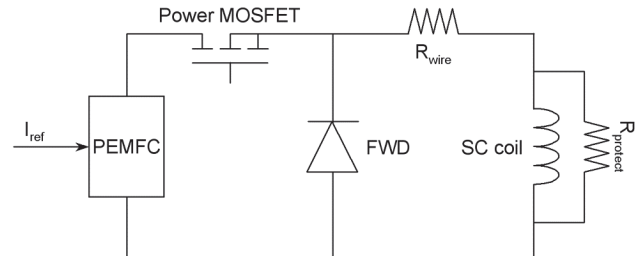


Fig. 5: “Electrical scheme of the superconducting coil current supply”

As previously, the cell is supplied with air and pure dry H₂. Cell temperature is regulated at 60 °C by a water cooling system. Inlet air temperature is 54 °C, and its relative humidity is approximately 75 %. Gas pressures are 1 atm at both sides. To ensure the FC operation as a current source over a large current range, the FC load resistance must be as low as possible. The power switch, a 100 V – 1200 A MOSFET, has been selected following this criterion. Indeed, its on-state resistance is about 1 mΩ when its gate is biased by a 15 V voltage source. As a result, the total resistance of the loop comprising the switch and the wires connecting the switch to the FC is close to 2 mΩ. The superconducting coil is cooled by liquid helium. The inductance value is 10 H. It is protected by a 0.7 Ω resistor (1 Ω at ambient temperature). The total resistance of connections between the coil and

the FWD is approximately 10 mΩ. A view of the experimental test bench is given in Fig. 6.

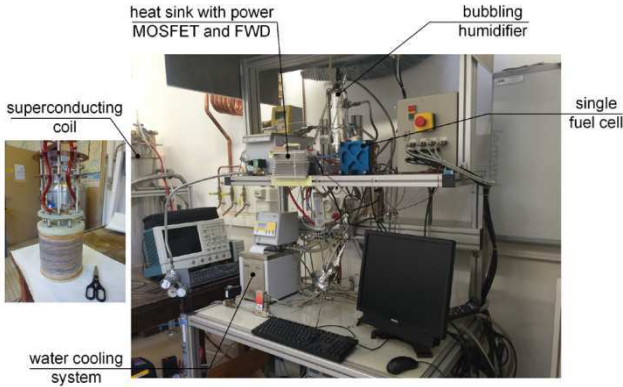


Fig. 6: “Experimental test bench. Right: FC system, left: superconducting coil outside the cryostat”

III.2. Controlling coil current by the H₂ flow rate

Fig. 7 hereafter presents the coil current (i.e. the current through the parallel association of the superconducting inductor and its protection resistor) and the FC voltage when simulating the connection of the coil to the FC, by turning-on the power switch. The FC is initially fed with gases, with the following setting: $I_{ref} = 20$ A, $\zeta_a = 1$, $\zeta_c = 4$. As it can be observed, the coil current is regulated in steady-state to the value corresponding to the H₂ flow rate. But in transient, the FC current source operation cannot be ensured because of the H₂ initially stored in the anode pipe. This leads to a current overshoot, then to a FC operation at negative voltage induced by the coil, when the current decreases to its steady state level. It can be noticed here that the negative voltage applied to the FC during this phase is limited by the FWD on-state voltage drop, to approximately -0.7 V if a PN diode is used, or -0.4 V if a Schottky diode is used. To avoid this kind of operation that may induce early aging of the cell, the circuit has to be closed before feeding the cell with gases. The second requirement to avoid negative voltage operation for the FC, is to limit the slope of H₂ flow rate variation, in order to remain in the voltage domain of current source operation for the FC.

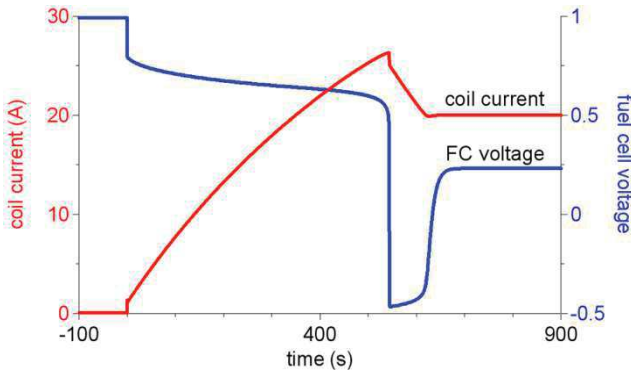


Fig. 7: “Simulated coil current and FC voltage at switch turn-on. Gas flow setting: $I_{ref} = 20$ A, $\zeta_a = 1$, $\zeta_c = 4$. FC supplied with gases before turn-on”

To illustrate this requirement, Fig. 8a shows coil current and FC voltage when simulating a step of gas

flow rates, from $I_{ref} = 20$ A to $I_{ref} = 30$ A (over-stoichiometry: $\zeta_a = 1$, $\zeta_c = 4$). Initially, the cell is operating in the current source mode, at 20 A. During current increase, as H₂ flow rate is higher than necessary for the actual level of current, the cell is overfed, so that it operates in normal mode. This results in a current overshoot, followed by a regime at negative voltage, as in the case of Fig. 7.

On the contrary, if H₂ flow rate is slowly increased, the FC stays in current source mode (Fig. 8b), which means that the current increase is controlled by H₂ flow rate. To obtain such a dynamic control, the H₂ variation flow rate, i.e. dI_{ref}/dt , must be low enough so that the corresponding transient inductance voltage, i.e. $L \times dI_{ref}/dt$, which is added to the circuit resistance voltage drops, has a level compatible with the FC operation as a current source. For example, the previous increase in coil current from 20 A to 30 A leads to a FC voltage equal to 360 mV in steady-state (i.e. $12 \text{ m}\Omega \times 30 \text{ A}$). If the increase is linearly operated within 1000 s, which corresponds to a transient inductance voltage of 100 mV (i.e. $10 \text{ H} \times 10 \text{ mA}\cdot\text{s}^{-1}$), the FC voltage is lower than 460 mV all over the current increase. Such low voltage level at a current density lower or equal to $0.3 \text{ A}\cdot\text{cm}^{-2}$ ensures current source operation for the FC, that is to say control of the application current by H₂ flow rate.

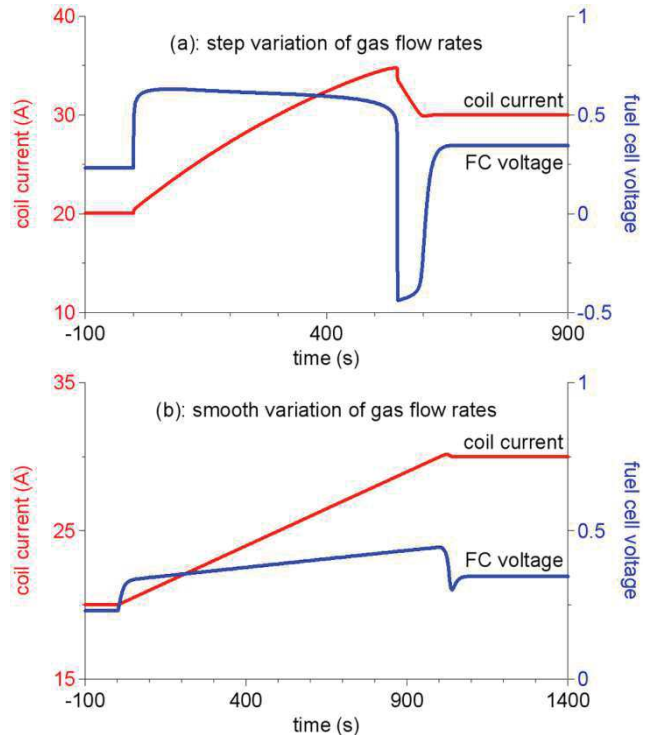


Fig. 8: “Simulated coil current and FC voltage for a transition of gas flow rates. Initial gas flow setting: $I_{ref} = 20$ A, $\zeta_a = 1$, $\zeta_c = 4$. (a): Step variation of gas flow rates. Step amplitude: $\Delta I_{ref} = 10$ A. (b): Smooth variation of gas flow rates. Gas flow variation: $\Delta I_{ref} = 10$ A, $dI_{ref}/dt = 10 \text{ mA}\cdot\text{s}^{-1}$ ”

To illustrate this example, Fig. 8b shows the coil current and the FC voltage when simulating a linear increase of gas flow rates, from $I_{ref} = 20$ A to $I_{ref} = 30$ A over 1000 s (over-stoichiometry: $\zeta_a = 1$, $\zeta_c = 4$). As previously in Fig. 8a, the cell is initially operating in the current source mode, at 20 A. It can be seen that

the coil current increases from 20 A up to 30 A at the expected rate, i.e. $10 \text{ mA}\cdot\text{s}^{-1}$. Nearly no current overshoot is observed, and the FC voltage remains positive all over the transient.

III.3. Experimental results

Fig. 9 presents the experimental coil current and the FC voltage obtained in the same conditions as in the simulation associated to Fig. 7 (i.e. at switch turn-on, the cell being initially fed with gases, with the following setting: $I_{ref} = 20 \text{ A}$, $\zeta_a = 1$, $\zeta_c = 4$). As previously for the simulation results, it can be seen that the coil current is regulated in steady-state at 20 A by H_2 flow rate, and that the transient response gives rise to a current overshoot, and to a FC operation at negative voltage when the current decreases to its steady-state level.

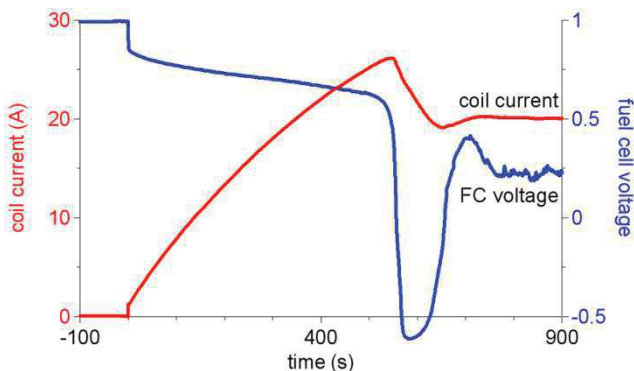


Fig. 9: “Experimental coil current and FC voltage at switch turn-on. Gas flow setting: $I_{ref} = 20 \text{ A}$, $\zeta_a = 1$, $\zeta_c = 4$. Fuel cell supplied with gases before turn-on”

Fig. 10a (experiment) hereafter is similar to Fig. 8a (simulation). It shows the experimental coil current and FC voltage when increasing suddenly gas flow rates from $I_{ref} = 25 \text{ A}$ to $I_{ref} = 30 \text{ A}$ (over-stoichiometry: $\zeta_a = 1$, $\zeta_c = 4$), the cell being initially in current source operating mode, at 25 A. The conclusions are the same than those deduced from simulation results depicted in Fig. 8a: it is necessary to limit the slope of H_2 flow rate variation, in order to control the current increase through the H_2 flow rate, and to avoid current overshoot and negative voltage operation for the FC. Fig. 10b and Fig. 11 demonstrate such a possible control by H_2 flow rate in transient. The first presents experimental results for an increasing linear transition of gas flow rates from $I_{ref} = 25 \text{ A}$ to $I_{ref} = 35 \text{ A}$, with a slope of $10 \text{ mA}\cdot\text{s}^{-1}$ (as in Fig. 8b). As obtained in simulation, the coil current increases with the expected slope, which means that it is actually controlled by the FC, through the H_2 flow rate. As a result, nearly no current overshoot is observed, and the FC voltage remains positive all over the transient. Fig. 11 also demonstrates possible effective current control by H_2 flow rate, but here during current decrease. In such a case, the transient inductance voltage induced by the variation of H_2 flow rate, i.e. $L \times dI_{ref}/dt$, is negative and may result in a negative voltage operation of the FC. It can be simply avoided by choosing, for the H_2 flow rate variation, a value for which the inductive term $L \times dI_{ref}/dt$ does not entirely compensate the circuit resistance voltage drops. In

the example of Fig. 11 that presents experimental results associated with a decreasing linear transition of gas flow rates from $I_{ref} = 35 \text{ A}$ to $I_{ref} = 25 \text{ A}$, the current slope limit is $-30 \text{ mA}\cdot\text{s}^{-1}$ (i.e. $-12 \text{ m}\Omega \times 25 \text{ A}/10\text{H}$). As the test was carried out with a slope of $-20 \text{ mA}\cdot\text{s}^{-1}$, it can be observed in Fig. 11 that the FC effectively operates in current source mode, with a positive voltage all over the transient.

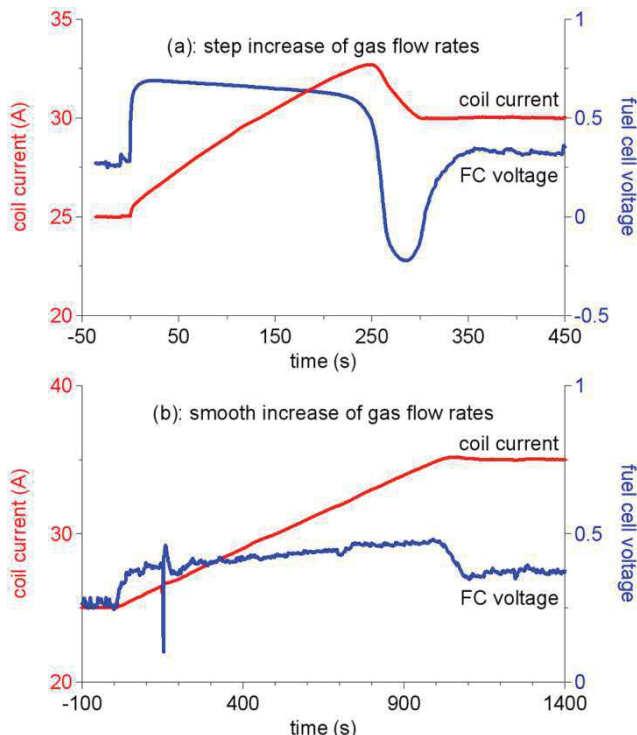


Fig. 10: “Experimental coil current and FC voltage for a transition of gas flow rates. Initial gas flow setting: $I_{ref} = 25 \text{ A}$, $\zeta_a = 1$, $\zeta_c = 4$. (a): Step variation of gas flow rates. Step amplitude: $\Delta I_{ref} = 5 \text{ A}$. (b): Smooth increase of gas flow rates. Gas flow variation: $\Delta I_{ref} = 10 \text{ A}$, $dI_{ref}/dt = 10 \text{ mA}\cdot\text{s}^{-1}$ ”

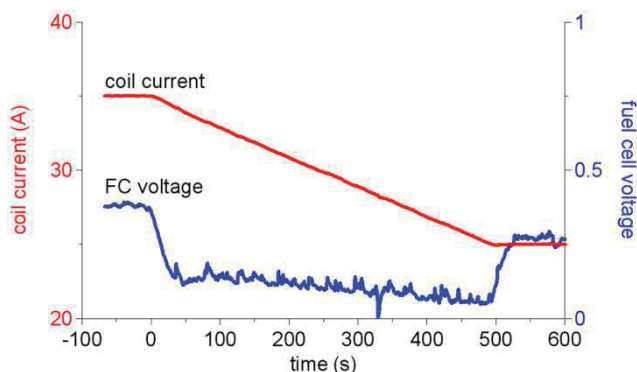


Fig. 11: “Experimental coil current and FC voltage for a slow decrease of gas flow rate. Initial gas flow setting: $I_{ref} = 35 \text{ A}$, $\zeta_a = 1$, $\zeta_c = 4$. Gas flow variation: $\Delta I_{ref} = -10 \text{ A}$, $dI_{ref}/dt = -20 \text{ mA}\cdot\text{s}^{-1}$ ”

IV. Conclusion

In this work, an original and innovating application of FC used as controlled current source has been highlighted, through supplying a huge inductance superconducting coil. This application has been first simulated in order to define requirements for an efficient current control by H_2 flow rate, as well as for

FC safe operation. It has been then experimented by carrying out a 100 cm² PEMFC and a 10 H superconducting coil cooled by liquid helium. To our state of knowledge, the application presented above seems totally novel since there can be found no literature source describing the use of FC operating as a current source controlled by H₂ flow rate, for supplying energy to power superconducting coils.

The interest of such an application is to provide an electric current in essence ready for use, i.e. responding to superconducting device constraints: direct current, generated at low voltage, free of detrimental harmonics or oscillations, independent from the grid, then not subject to grid power failures. High current level can be simply reached in theory, by connecting single cells in parallel, or by increasing the active surface of the electrochemical generator. For this purpose, further works have to be led to assess the feasibility of these techniques at high current level: controlling current by H₂ flow rate when paralleling several single fuel cells, investigating current density distribution when operating a large (several hundreds of cm²) single FC as a current source.

Acknowledgements

We would like to acknowledge the cryogenic centre of the IJL institute (Institut Jean Lamour), and more especially Thomas Hauet for allowing us to carry out these experiments in the research centre, and Luc Moreau for his help during experimental tests.

Nomenclature

a	: Water activity (-)
A	: Active surface (m ²)
c	: Concentration (mol.m ⁻³)
C	: Capacitor (F)
D	: Diffusion coefficient of species (m ² .s ⁻¹)
E	: Equilibrium potential (V)
F	: Faraday's constant, 96472 (C.mol ⁻¹)
HR	: Relative humidity (-)
j ₀	: Exchange current density (A.m ⁻²)
J	: Molar flow (mol.s ⁻¹)
I	: Current (A)
nd	: Electro-osmotic drag coefficient (-)
P	: Pressure (Pa)
R	: Gas constant, 8.314 (J.mol ⁻¹ .K ⁻¹)
t	: Time (s)
T	: Temperature (K)
V	: Voltage (V)
x	: 1D coordinate (m)
X	: Proton exchange capacity (mol.kg ⁻¹)
Greek letters	
α	: Transfer coefficient (-)
δ	: Layer thickness (m)
ε	: Porosity (-)
η	: Surface overvoltage (V)
λ	: Membrane water content (-)
ζ	: Stoichiometry coefficient (-)
ρ	: Density (kg.m ⁻³)
σ	: Electrical conductivity (S.m ⁻¹)
φ	: Electrical potential (V)

Subscripts

a	: Anode
c	: Cathode
cell	: Fuel cell
dl	: Double layer
eff	: Effective value
hum	: Humidifier
in	: Inlet
i, j	: Species (H ₂ , O ₂ , H ₂ O, N ₂)
m	: Membrane
ref	: Reference condition
s	: Electronic phase
sat	: Saturated value
sorp	: Sorption

References

- Andujar J. M., Segura F., Vasallo M. J., A suitable model plant for control of the set fuel cell DC/DC converter, *Renewable Energy*, 33, 813-826, (2008).
- Bonnet C., Lopicque F., Belhadj M., Gerardin K., Raël S., Hinaje M., Mitchell L., Goldsmith V., Kmietek S. J., Can PEM fuel cells experience appreciable degradation at short circuit ?, *Fuel Cell*, available online, (2016).
- Chiu L. Y., Diong B., Gemmen R. S., An improved small-signal model of the dynamic behaviour of PEM fuel cells, *IEEE Transactions on Industry Applications*, 40, 970-977, (2004).
- Fontès G., Turpin C., Astier S., A large signal and dynamic circuit model of a H₂/O₂ PEM fuel cell: description, parameter identification and exploitation, *IEEE Transactions on Industrial Electronics*, 57, 1874-1881, (2010).
- Hinaje M., Berger K., Lévêque J., Davat B., Superconducting coil fed by PEM fuel cell, *International Journal of Hydrogen Energy*, 38, 6773-6779, (2013).
- Hinaje M., Nguyen D. A., Raël S., Davat B., Bonnet C., Lopicque F., 2D modelling of a defective PEMFC, *International Journal of Hydrogen Energy*, 36, 10884-10890, (2011).
- Hinaje M., Raël S., Caron J.-P., Davat B., An innovating application of PEM fuel cell: current source controlled by hydrogen supply, *International Journal of Hydrogen Energy*, 37, 12481-12488, (2012).
- Lazarou S., Pyrgioti E., Alexandridis A. T., A simple electric circuit model for proton exchange membrane fuel cells, *Journal of Power Sources*, 190, 380-386, (2009).
- Noiyng P., Hinaje M., Thounthong P., Raël S., Davat B., Using electrical analogy to describe mass and charge transport in PEM fuel cell, *Renewable Energy*, 44, 128-140, (2012).
- Page S. C., Anbuky A. H., Krumdieck S. P., Brouwer J., Test method and equivalent circuit modeling of a PEM fuel cell in a passive state, *IEEE Transactions on Energy Conversion*, 22, 764-773, (2007).
- Yu D., Yuvarajan S., Electronic circuit model for proton exchange membrane fuel cells, *Journal of Power Sources*, 142, 238-242, (2005).